

## Structural properties of Haeckelite nanotubes

Ph Lambin<sup>1</sup> and L P Biró<sup>2</sup>

<sup>1</sup> Département de Physique, Facultés Universitaires N. D. de la Paix,  
61 Rue de Bruxelles, B 5000 Namur, Belgium

<sup>2</sup> Research Institute for Technical Physics and Materials Science,  
H-1525 Budapest, PO Box 49, Hungary

E-mail: [philippe.lambin@fundp.ac.be](mailto:philippe.lambin@fundp.ac.be)

*New Journal of Physics* **5** (2003) 141.1–141.14 (<http://www.njp.org/>)

Received 9 July 2003

Published 20 October 2003

**Abstract.** The name ‘Haeckelite’ has been proposed to designate a three-fold coordinated network generated by a periodic arrangement of pentagons, hexagons and heptagons (Terrones H *et al* 2000 *Phys. Rev. Lett* **84** 1716). Starting from a planar Haeckelite array, tubular structures are obtained by applying the same wrapping procedure as for the usual nanotubes, which are rolled up sheets of graphene. This paper is a short review of the structural properties of Haeckelite nanotubes, as investigated by computer molecular modelling. The Haeckelite nanotubes may adopt various shapes, among which coiled structures, double-screw molecules, corrugated cylinders, and pearl-necklace-like nanotubes are the most spectacular. It is shown that some of these structures may explain exotic forms of C nanostructures revealed by electron microscopy on samples produced experimentally. The identification of the possible Haeckelite structure of a nanotube by electron diffraction and scanning tunnelling microscopy is discussed.

### Contents

<b>1</b>	<b>Introduction</b>	<b>2</b>
<b>2</b>	<b>Haeckelite network</b>	<b>3</b>
<b>3</b>	<b>Atomic structure</b>	<b>4</b>
<b>4</b>	<b>Discussion</b>	<b>8</b>
<b>5</b>	<b>Conclusion</b>	<b>13</b>
	<b>Acknowledgments</b>	<b>13</b>
	<b>References</b>	<b>13</b>

## 1. Introduction

Haeckelite carbon nanotubes are structures obtained by rolling up a flat and periodic three-coordinated network containing an equal number of pentagons and heptagons, and an arbitrary number of hexagons [1]. These are interesting systems that have been proposed theoretically a few years after the prediction that a graphitic planar structure composed exclusively of pentagons and heptagons could be metallic [2].

Pentagon and heptagons are important structural defects in carbon nanostructures [3]. Pentagons are certainly present in fullerenes and carbon onions [4], in nanotube caps [5], nanocones [6], and in the conical cap of nanohorns [7]. The presence of heptagons is suspected in some negatively-curved parts of multiwall nanotubes [5, 8] and in ideal Y-type tube connections [9]. Pentagons and heptagons are very often grouped in pairs [10, 11] or in the form of Stone–Wales defects [12], which are associations of two such pairs.

The presence of pentagon–heptagon pairs, and more specifically Stone–Wales defects, in nanotubes is highly suspected, perhaps at a level of one part per hundred [13], although no direct observation can testify for this. Pentagon–heptagon pairs are also required to interconnect two nanotubes with different chiralities [10, 14]. In these intramolecular junctions, signatures of the defects have been revealed by scanning tunnelling microscopy and spectroscopy [15, 16]. A large number of pentagons and heptagons is actually involved in the structure of ideal helical nanotubes [11, 17]. In fact, helical structures can be produced at high yield by catalytic chemical vapour deposition (CVD) [18, 19]. The problem is to explain how pentagons and heptagons can be incorporated so regularly in the structure during the nanotube growth process [20], in order to generate such a regular pitch and diameter of the helix.

As an alternative to the periodic insertion of pentagons and heptagons in the construction of honeycomb tori and helices, László and Rassat [21] have proposed to start with planar patterns of azulene units, which are fused pentagon–heptagon pairs. Rolling up a stripe of azulenes, possibly mixed with hexagons, leads to a tube that automatically bends and may close itself in a torus, which is a particular case of a helix with zero pitch. This construction is similar to the one used to generate straight Haeckelite nanotubes [1]. Recently, this idea was generalized by assembling more complex patterns of azulenes and hexagons in a planar sheet, and wrapping the obtained Haeckelite-like stripes [22]. It was shown that specific wrappings lead to a new variety of toroidal, coiled, screw-like and pearl-necklace-like structures [22, 23]. These structural shapes appear naturally and they do not demand the insertion of additional odd-membered polygons. The building blocks are azulene and hexagonal units in proportions that can vary at will. In some exotic forms of C nanotubes produced by CVD, it is possible that a high concentration of pentagons and heptagons are indeed incorporated in the structure, as the result of both fast kinetic and low synthesis temperature, leading to metastable states that cannot anneal out easily. It is indeed believed that at the lower synthesis temperatures, newly incorporated pentagon–heptagon pairs cannot easily transform into two hexagons. Alternatively, Haeckelite nanotubes might possibly be produced by a rearrangement of the atoms of a nanotube after irradiation. In particular, the transformation of a single-wall nanotube in a necklace-like object of the kind discussed here below has been observed after strong irradiation of the sample in a transmission electron microscope [24].

In the large majority of cases, a Haeckelite structure cannot be obtained from a regular nanotube solely by Stone–Wales bond rotations, which transform four adjacent hexagons into two pentagons and two heptagons. However, the Haeckelite structures explored so far do involve

adjacent pentagon–heptagon pairs. These azulene units act as disclinations of opposite signs that do not induce a sharp and permanent bend of the structure, as opposed to isolated pentagons and heptagons that would do so [25]. The azulene units are edge dislocations [26], and these dislocations may glide under appropriate tensile stress of the nanotube. This gliding, which proceeds by successive rotations of a CC bond, might release part of the strain accumulated in the Haeckelite nanotube [27]. By applying a tensile strain, the azulene units could move along the structure [28], but they will not anneal out unless two azulenes corresponding to opposite Burgers vectors meet each other, forming thereby a Stone–Wales defect which could disappear by back-transformation of the defect in four hexagons.

## 2. Haeckelite network

Haeckelite tubular structures are constructed from two-dimensional (2D) periodic arrays of pentagons, hexagons and heptagons, in the same way as for graphene nanotubes, by rolling up the sheet into a seamless cylinder [1]. Three models of Haeckelites structures were proposed earlier [1]. These models were based on the following periodic flat patterns: (1) a rectangular unit cell with four azulenes and no hexagon; (2) a hexagonal unit cell with three azulenes and two hexagons; (3) an oblique unit cell with two azulenes and two hexagons. The nanotubes generated from these periodic arrays were found to be straight, possibly slightly buckled, tubes.

In a previous paper [22], Haeckelite-like patterns were generated by starting from an azulenoid stripe proposed by László and Rassat [21], where pentagon–heptagon pairs are joined head to tail, and by inserting a certain number of hexagons in between. The process is illustrated in figure 1 for the insertion of three hexagons between the two azulene units, shown by shaded surfaces. This pattern is reproduced periodically in the plane, with unit vector  $\vec{a}_1$  and  $\vec{a}_2$ . The structure was optimized in two dimensions, including the shape and dimensions of the unit cell. All the structural optimizations described in this paper were performed with the empirical Brenner–Tersoff potential [29, 30]. The length of the unit vectors is  $a_1 = 0.70$  nm and  $a_2 = 0.52$  nm, and the angle between them is  $97.8^\circ$ . All the CC bonds have approximately the same length, but the bond angles are distorted. This means that the 2D sheet is strongly strained. It has an energy of 0.54 eV/atom above graphene and is very unstable against an out-of-plane relaxation. When relaxed in three dimensions, the structure of figure 1 starts rolling and curling to release its strain. For instance, out-of-plane relaxation of a  $6 \times 8$  (figure 1 is  $8 \times 8$ ) superstructure with periodic boundary conditions applied in 2D lowers the energy of the Haeckelite pattern to 0.32 eV/atom.

The distortion needed for the strictly 2D representation is easily removed, when the three-dimensional structure, wrapped from the Haeckelite sheet, is allowed to relax. The rich variety of tubular structures generated by the Haeckelite pattern discussed above finds its origin in the metastable state of the 2D structure. One of the likely reasons for the non-stability of this 2D structure is the existence of pentagon–pentagon pairs. In figure 1, the bonds shared by two adjacent pentagons are highlighted by heavy dots. These bonds have been called *stressors* [23], because in all the tubular structures generated from the 2D pattern those bonds were found to be placed in regions with strong local curvature, and consequently high stress. The unit cell contains one such stressor. In the nanotube, the stressors generate regions of protruding (positive stressor) or dipping (negative stressor) local curvature, which can spiral around the tube. Another interesting property of the Haeckelite network used here is the existence of heptagon–heptagon pairs arranged in zig-zag patterns. One of these is visualized by the thin zig-zag line in figure 1.

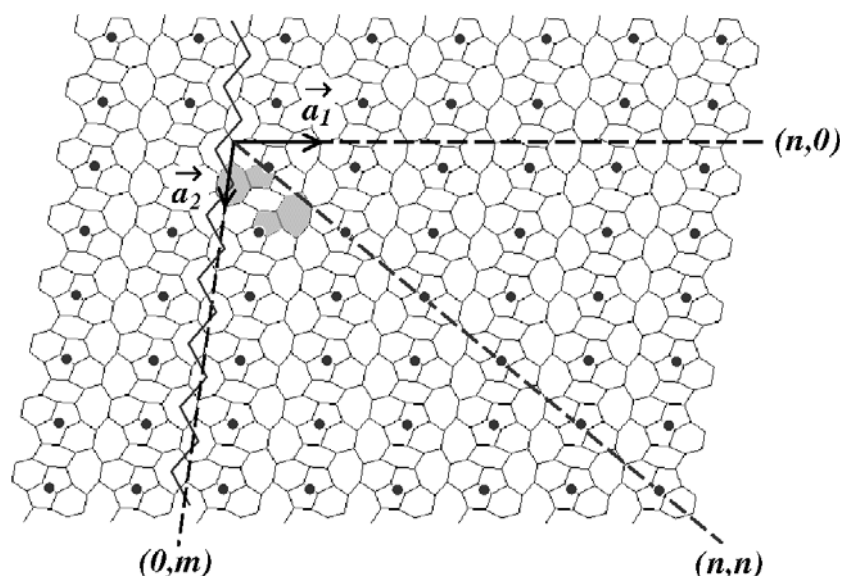


**Figure 1.** Planar periodic network containing two azulene units (shaded surfaces) and three hexagons. The primitive vectors  $\vec{a}_1$  and  $\vec{a}_2$  are indicated in the drawing, together with the circumferential directions corresponding to  $(n, 0)$ ,  $(n, n)$ , and  $(0, m)$  wrappings. The thin zig-zag line along  $\vec{a}_2$  connects the centres of adjacent heptagons. On both sides, there are pairs of pentagons whose common edges are marked by black dots. These bonds form the so-called ‘stressors’ discussed in the text.

These rows of heptagons are separated by stressor lines. They generate regions with negative Gaussian curvature in the nanotube.

### 3. Atomic structure

Stripes of the Haeckelite-like 2D network shown in figure 1 were rolled up following the usual wrapping procedure used for graphitic nanotubes. In this construction, the site at the origin of the primitive vectors  $\vec{a}_1$  and  $\vec{a}_2$  is superimposed on the site located at  $\vec{C}_h = n\vec{a}_1 + m\vec{a}_2$ . The atomic structure of the perfectly cylindrical  $(n, m)$  nanotube so obtained was then fully relaxed with a conjugate-gradient algorithm, using the Brenner–Tersoff potential. Apart from screw operations, the nanotube has no symmetry operation. As illustrated in the next section, strong reconstruction of the tubular structure may take place upon relaxation, which, in general, does not conserve the helical symmetry of the starting cylindrical molecule. This means that a rather long portion of the molecule needs to be considered. Nanotubes of at least 4.5 nm in length (before relaxation) were generated with open ends. After structural optimization, the energy was computed and averaged over all the three-fold coordinated atoms. In this way, the effects of the dangling bonds at both ends on the energetics of the structure were minimized. The energy results are listed in table 1, which also gives the energy,  $\Delta E = E - E_0(d)$ , above that of a graphene nanotube having the same diameter  $d$  as the original perfect cylindrical Haeckelite structure. The energy of the usual single-wall nanotubes obtained with the Brenner–Tersoff potential is well represented by the following law [31]:  $E_0(d) = A/d^2 + B/d^3$ , where the zero

**Table 1.** Wrapping indices  $(n, m)$ , tube diameter before relaxation  $d$ , energy above graphite after relaxation  $E$ , and the excess of energy compared to a graphene nanotube with identical diameter  $\Delta E$  for the Haeckelite tubular structures illustrated in this paper.

$(n, m)$	$d$ (nm)	$E$ (eV/atom)	$\Delta E$ (eV/atom)
(0, 3)	0.499	0.30	0.12
(0, 4)	0.665	0.32	0.21
(0, 5)	0.831	0.26	0.20
(0, 6)	0.997	0.28	0.24
(1, 0)	0.223	1.00	$\sim 0$
(2, 0)	0.446	0.56	0.33
(3, 0)	0.669	0.46	0.35
(4, 0)	0.892	0.38	0.32
(1, 1)	0.259	0.68	$\sim 0$
(2, 2)	0.519	0.42	0.24
(3, 3)	0.778	0.40	0.32
(4, 4)	1.038	0.33	0.29
(2, -2)	0.591	0.35	0.22
(2, -1)	0.497	0.46	0.28
(2, 1)	0.454	0.55	0.32
(2, 3)	0.622	0.32	0.21

of energy is that of flat graphene, with  $A = 0.042\,1288\text{ eV nm}^2$  and  $B = 0.002\,145\,52\text{ eV nm}^3$ . This formula is valid for  $0.4 < d < 1.5\text{ nm}$ . Table 1 shows that, for very small diameters, the Haeckelite and the graphene nanotubes have about the same energy (the values of  $\Delta E$  given in table 1 for  $d < 0.4\text{ nm}$  are not reliable, but they are much less than  $0.1\text{ eV/atom}$ ). When  $d$  is larger than  $0.6\text{ nm}$ ,  $\Delta E$  ranges between  $0.20$  and  $0.35\text{ eV/atom}$  in favour of the graphene nanotube. These values compare well with the energy of  $0.32\text{ eV/atom}$  of the out-of-plane relaxed periodic pattern (see above).

Some of the optimized Haeckelite nanotubes are illustrated in this section. The simplest nanostructures to start with are the nanotubes of the family  $(0, m)$  shown in figure 2. Here, the wrapping vector  $\vec{C}_h$  is parallel to the zig-zag chains of heptagons (see figure 1). In addition, there are also lines of stressors running parallel to the  $(0, m)$  direction in the planar development. In the rolled-up structure, the stressor lines parallel to  $\vec{C}_h$  lead to protruding rings, which are separated by annular grooves formed by the heptagon chains. The repeat distance between the protruding rings is approximately the same for all the  $(0, m)$  nanotubes, around  $0.65\text{ nm}$ , slightly less than  $a_1$ . As indicated by table 1, the  $(0, m)$  family is characterized by a small strain energy. All nanotubes of that kind were found to be robust against deformation; the tube radius could be increased without generating strange and complex shapes. The shape adopted by all these nanotubes is that of a necklace of pearls. Since they have the same structure, the  $(0, m)$  nanotubes can be placed inside one another. Multiwall necklace structures can therefore be generated in this way [32]. The inter-layer distance of  $0.34\text{ nm}$  demands that the  $m$  index increases by steps of 4 units. Multiwall necklace structures have been observed experimentally

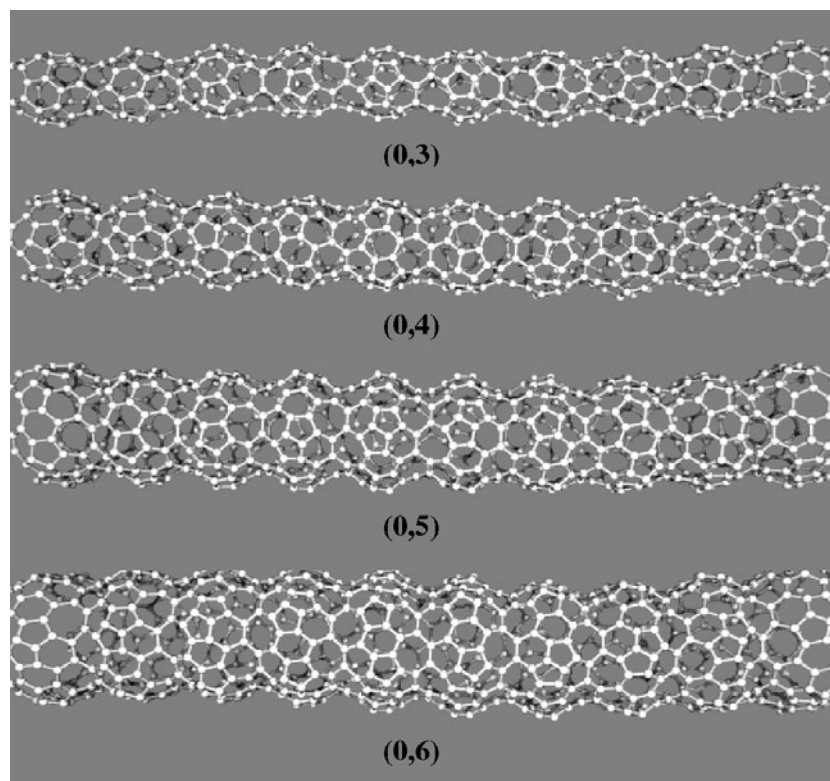


**Figure 2.** Ball-and-stick representations of  $(0, m)$  nanotubes generated from the Haeckelite stripe of figure 1 for  $m = 3, 4, 5$  and  $6$ .

(see next section), with bigger ‘pearls’ than here. In connection with that observation, it would be possible to increase the distance between the protruding rings in the structural models of figure 2, by inserting additional rows of hexagons between the zig-zag chains of heptagons and the stressor lines in the 2D network shown in figure 1.

The overall curvature of the tubular Haeckelite structures arises from the asymmetric way in which the stressors are distributed in their unit cell. It is reasonable to admit that the structure adopts a shape in which the stress is evenly distributed all over the structure. One may observe in figure 1 that, when the wrapping indices are of the particular kinds  $(n, 0)$  and  $(n, n)$ , the stressors in the unit cell are arranged in lines parallel to the wrapping vector. This was also the case with the  $(0, m)$  nanotubes. But in  $(n, 0)$  and  $(n, n)$  nanotubes, unlike with the  $(0, m)$  family, the zig-zag chains of heptagons are not parallel to the circumferential direction. In the planar development, these zig-zag chains form an angle  $\theta = 8^\circ$  with respect to the axis of the  $(n, 0)$  nanotubes and  $32^\circ$  in the  $(n, n)$  configuration. These chains become helices in the rolled-up structure. The two families of nanotubes  $(n, 0)$  and  $(n, n)$ , illustrated in figures 3 and 4, respectively, have similarities. When present, the asymmetry created by the stressors can be partly compensated by stressing opposite regular bonds. An example is the  $(1, 0)$  nanotube, which adopts the shape of a nice regular helix. It contains only one stressor around its circumference. In the 2D development, the stressors form a line not parallel to the axis, and this line becomes a helix in the rolled-up nanotube, with the same pitch angle  $\theta$  as the zig-zag chain of heptagons. As a result, the structure coils. Another similar example is the  $(1, 1)$  nanotube (figure 4). The pitch of these two helical

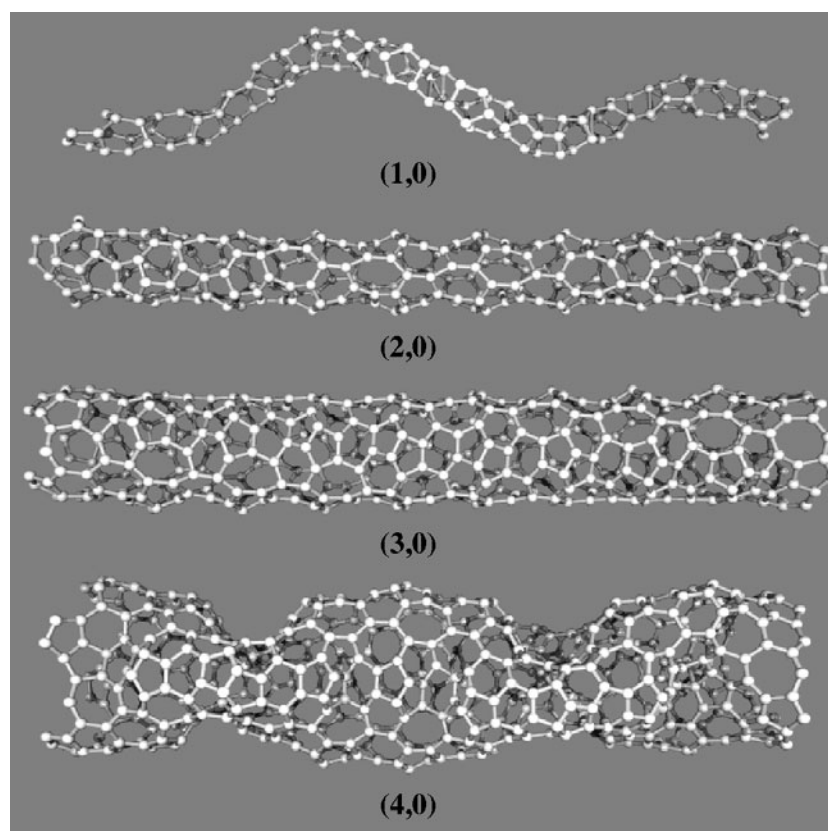


**Figure 3.** Ball-and-stick representations of  $(n, 0)$  nanotubes generated from the Haeckelite stripe of figure 1 for  $n = 1, 2, 3$  and 4.

molecules is of the order of that of a helix drawn by the stressor line on the cylinder, namely  $C_h / \tan \theta$ , equal to 5.0 for  $(1, 0)$  and 1.3 nm for  $(1, 1)$ . Due to its smaller pitch, the latter shows a much smaller degree of curvature than the former, and is a ‘curled’ nanotube [22].

The  $(2, 0)$  and  $(3, 0)$  nanotubes are straight nano-objects. Here, there are two and three stressor lines, respectively, arranged in a way that they equilibrate each other. The same holds true for  $(2, 2)$  and  $(3, 3)$  (figure 4). In  $(2, 2)$ , the two stressor lines form two slightly protruding features that spiral around the tube in opposite phases. They are separated by continuous grooves that also spiral around the structure, with a pitch approximately twice that of  $(1, 1)$ . This molecule is a double-screw structure, like the one discussed in [22] (see below). An interesting feature worth pointing out for  $(4, 0)$  is the occurrence of negative stressors, i.e. apparent cavities where pentagon–pentagon pairs are found. In fact, these cavities are the results of a flattening of the molecule, where its cross section has an elliptical shape which is viewed along its long axis in figure 3. Slightly away from there, the cross section transforms progressively in a circle and in an ellipse again, rotated by approximately  $90^\circ$  and now viewed along its short axis (as in the central part of the  $(4, 0)$  model shown in figure 3). This alternation continues all along the molecular axis, so that the molecule looks like a necklace in projection. Here, the pearls resemble elongated ellipsoids which rotate successively by  $\sim 90^\circ$  about the molecular axis. A somewhat similar feature is found in  $(4, 4)$  (see figure 4), with however an even stronger flattening. The cross section of this tubular molecule is like an ellipse squeezed along its short axis, like a ‘8’.

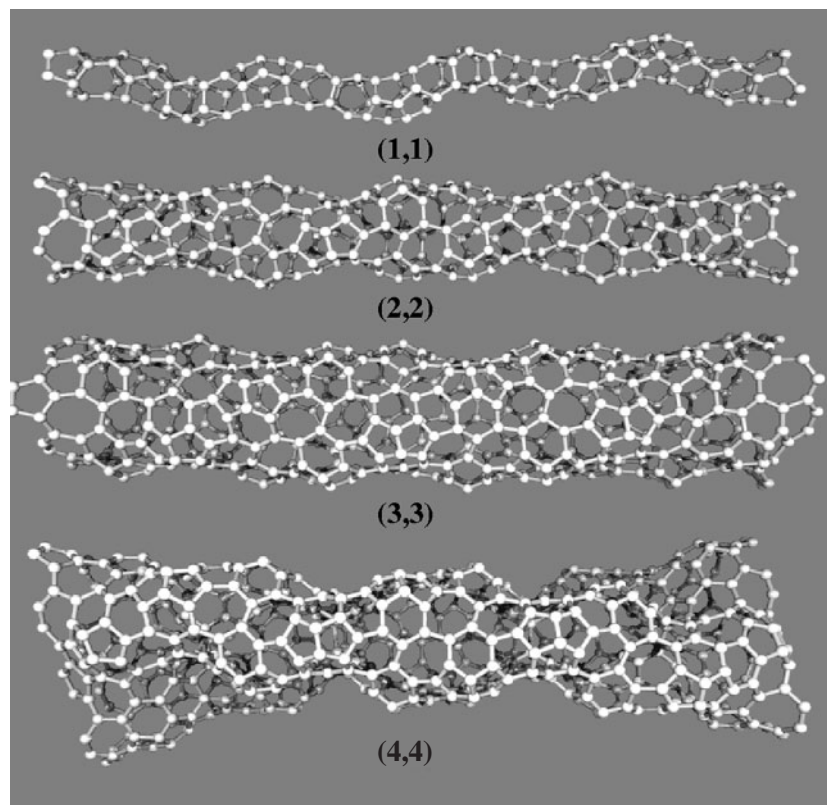


**Figure 4.** Ball-and-stick representations of  $(n, n)$  nanotubes generated from the Haeckelite stripe of figure 1 for  $n = 1, 2, 3$  and 4.

The strongest curvature is where the stressors are. The structure looks like a twisted ribbon, with  $2\pi$  twist taking place over a length of about 4.5 nm. In spite of its intricate shape, this molecule has a rather low penalty energy (see table 1).

In figure 5, the structures of four nanotubes with wrapping indices of the kind  $(2, m)$  are compared.  $(2, -2)$ ,  $(2, -1)$ , and  $(2, 3)$  are both double-screw nanotubes, like  $(2, 2)$ . In these molecules, the two stressor lines protrude outward and spiral around the nanotube. The grooves between them, with negative Gaussian curvature, are formed by the zig-zag rows of heptagons. The pitch of the screws in these three molecules is 2.1, 2.3, and 2.0 nm, respectively. In  $(2, 1)$ , there are also two stressor lines. In the planar development of the structure (figure 1), the angle between the tube axis and the stressor lines is much smaller than for the three previous molecules,  $13^\circ$ , and is comparable to that realized in  $(2, 0)$ . And indeed,  $(2, 1)$  and  $(2, 0)$  have similar structural characteristics; both of them are straight, slightly buckled nanotubes.

#### 4. Discussion

As mentioned in the introduction, carbon nanotubes may adopt a large variety of shapes depending on the synthesis technique used and the growth conditions. In parallel with this well-known observation, Haeckelite tubular structures present a rich variety of shapes. Only a very few examples have been explored up to now by computer modelling. All of the structures illustrated

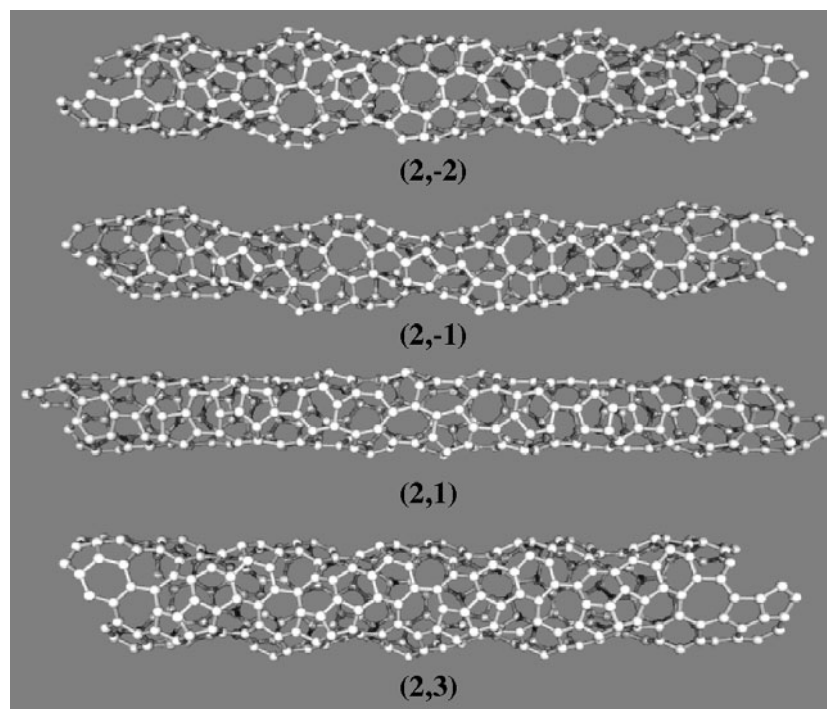


**Figure 5.** Ball-and-stick representations of  $(2, m)$  nanotubes generated from the Haeckelite stripe of figure 1 for  $m = -2, -1, 1$  and  $3$ .

in the previous section were obtained with the same 2D array of pentagons, hexagons and heptagons. This Haeckelite pattern may generate coil, double-screw and necklace structures, and all of them have been observed experimentally. Other Haeckelite patterns have been investigated recently by László and Rassat [33], who considered various planar tilings where the pentagons and heptagons are separated from each other by hexagons. After wrapping into a cylinder and structural relaxation, these patterns can also generate torus and helical nanotubes.

There have been numerous reports on the synthesis of coiled nanotubes by catalytic CVD since their first observation by high-resolution transmission electron microscopy (TEM) [34]. Most frequently, the coiled structures are observed when using a growth temperature around  $700^\circ\text{C}$ , or lower. High-temperature methods, like the electric-arc discharge, produce mainly remarkably straight, well-graphitized nanotubes, while the typical products of the CVD method consist of randomly curved tubes, or bundles of tubes in which some ordering of the curled tubes may be observed. The random or regular curvature, and the poor graphitization of the CVD tubes, as compared with the ones grown by arc discharge, can be attributed to a relatively high number of non-hexagonal rings in the CVD structures. The *ad hoc* explanation of the observed coiled structure is the regular incorporation of pentagon and heptagon pairs placed at opposite sides [11, 17], which bend the structure at an angle of  $30^\circ$ – $40^\circ$  [35]. Indeed, on some occasions, a polygonal shape has been observed when imaging a coiled carbon nanotube along its axis in a TEM [36]. The polygonal projection of the structure in a plane perpendicular to its axis indicates sharp bending of the coil at each pentagon–heptagon pair. This construction, based on a regular insertion of separated pentagons and heptagons in the honeycomb network [37], is not incompatible with the Haeckelite model [33].

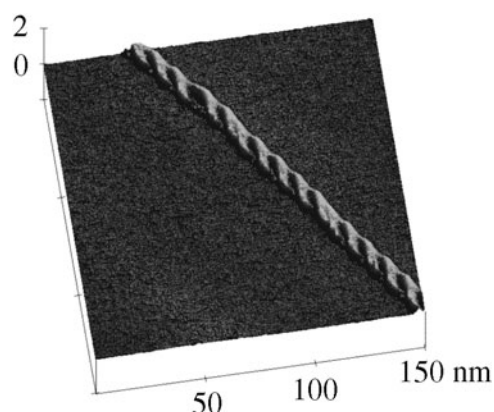


**Figure 6.** Experimental STM 3D representation of a double-screw multiwall nanotube [22].

Regularly coiled tubes may be produced when the growing nanotube nucleus achieves a suitable proportion of pentagon–heptagon pairs and hexagons, with an arrangement that can generate a structure like the ones described above. The (1, 0) and (1, 1) Haeckelite systems are coiled and ‘curled’ nanotubes. Of course, the diameter is so small that these structures must be unstable. Nevertheless, they indicate that a Haeckelite pattern with fused pentagon–heptagon pairs may generate helical tubular molecules. It is very likely that other patterns than the one displayed in figure 1 will also generate coiled tubes. By increasing the proportion of hexagons, coiled nanotubes with a larger diameter than realized here should be generated.

Figure 6 shows an experimental STM image in which a double helix is seen, which extends over several hundreds of nanometres. Given the diameter of the molecule, as estimated from its overall height above the graphite support that holds it in place, it is a multiwall nano-object. If the structure were built of two, independent, but intercoiled nanotubes like in multiple-strand coiled nanoropes [19, 38, 39], the STM topography would look different, due to the particular tunnelling conditions at the points where the two tubes cross each other under the STM tip. Structural models, agreeing with that observation, are the double-screw structures generated by the (2, –2), (2, –1) and (2, 2) Haeckelite nanotubes. Here again, the diameter and pitch distance of the molecular models do not agree at all with the experimental observations. But again, this is due to the very large proportion of non-hexagonal rings used in the Haeckelite pattern. By increasing the number of hexagons, multiple-screw structures with more realistic dimensions could probably be generated.

Pearl-necklace-like nanotube structures have been found in samples produced by high-pressure carbon evaporation [40]. The observed necklace structure is an assembly of hollow, rather spherical structures typically composed of eight concentric graphitic layers. A continuous outer shell made of  $\sim 10$  graphitic layers surrounds the spherical objects, which are encapsulated in this nanotube mantle. A single-wall representation of a ‘spherically modulated’ nanotube, such as is observed in the pearl mantle shell, is provided by the necklace structures of figure 2. Again, the dimensions of the Haeckelite necklaces do not agree with the observed structures, which have a diameter of about 100 nm. Nanotubes having a similar pearl-necklace structure have also been discovered in samples produced by plasma evaporation of graphite in the presence of transition metal catalysts [32]. Figures 7(a) and (b) are SEM and TEM pictures of such a

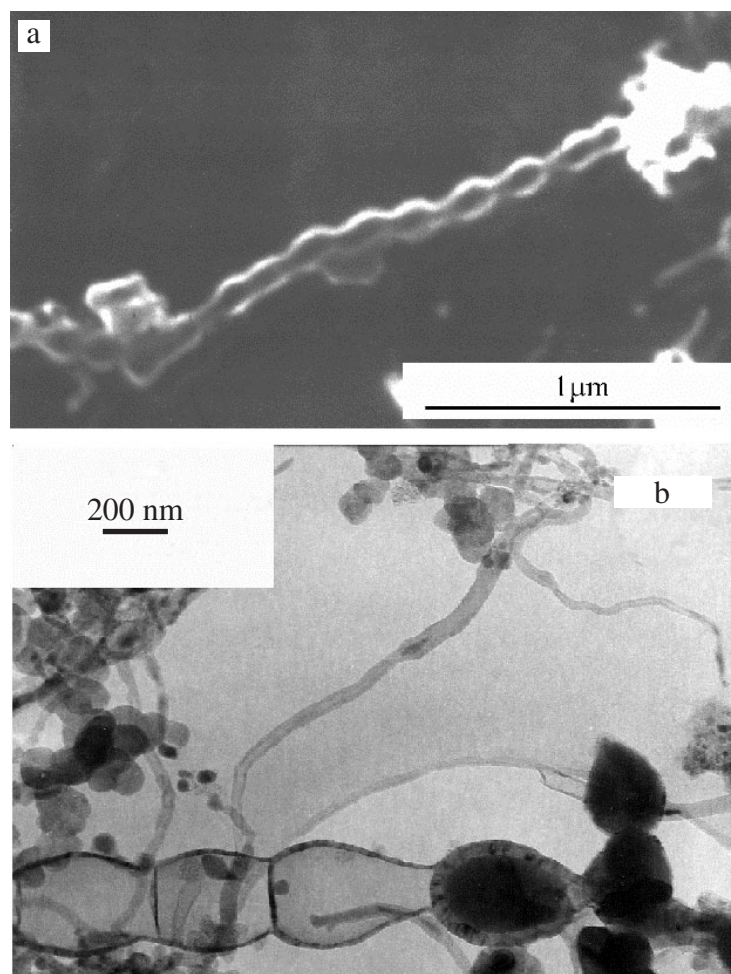


**Figure 7.** (a) SEM and (b) TEM pictures of a necklace multiwall nanotube produced by carbon evaporation in an AC plasma reactor, in the presence of a mixture of Ni, Co, Y used as catalyst [32].

necklace structure. Both SEM and TEM images clearly reveal that the necklace-type structures are built from a succession of balls, which seem to be curved without any external constraint. The ball-like objects are hollow, except the rightmost one in the necklace of figure 7(b), which is clearly filled and has a much thicker wall than the other pearls. High-resolution TEM [32] revealed an arrangement of the atomic layers similar to that reported in [40], namely that the pearls are surrounded by continuously curved and somewhat crumbled graphitic layers. It is proposed that this curvature and crumbling are manifestations of the Haeckelite-type arrangement of the carbon atoms.

The important question is of course whether it would be possible to clearly identify a Haeckelite structure experimentally. Selected-area electron diffraction and STM might be adequate techniques for that purpose.

Electron diffraction patterns of two Haeckelite nanotubes are shown in figure 8. They were computed with the kinematical theory, which is known to produce a reliable description of the diffraction intensities produced by carbon nanotubes [41]. For these calculations, the atomic coordinates of long Haeckelite nanotubes are required to avoid finite-size effects. Nanotubes

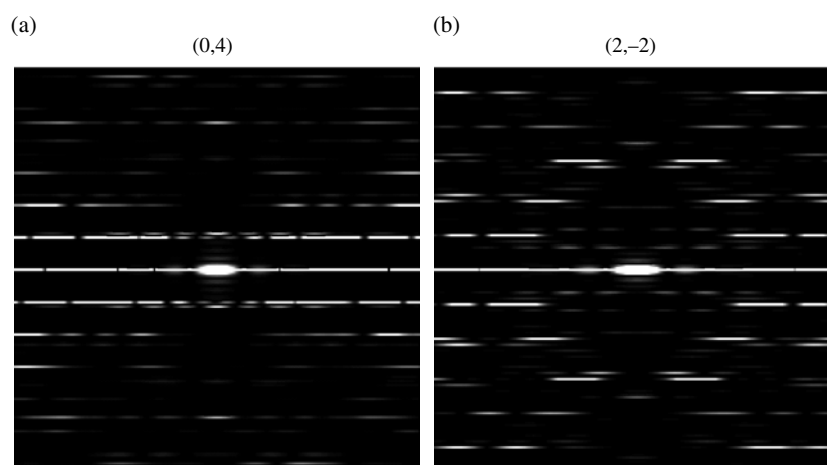


**Figure 8.** Computed electron diffraction pattern of the (0, 4) (a) and (2,  $-2$ ) (b) Haeckelite nanotubes. The vertical direction is parallel to the nanotube axis. The scattering wavevector ranges from  $-5.2$  to  $+5.2 \text{ \AA}^{-1}$  in both horizontal and vertical directions.

with infinite length were obtained by reproducing periodically a  $\sim 5$  nm long tube section, whose structure was relaxed with periodic boundary conditions. The length of the period was chosen in such a way that the rolled-up Haeckelite sheet became periodic after the application of a small axial twist. As expected, the computed diffraction patterns of the Haeckelite nanotubes do not resemble the one generated with graphene nanotubes. In particular, there is no hexagonal arrangements of spots around the central (0, 0) beam. Also, there is little intensity modulation along the central horizontal line. With a perfect cylindrical tube, the intensity modulation along this line is controlled by the reciprocal value of the cylinder radius. Here, the radius is not constant due to the corrugated shape of the Haeckelite structure. The diffraction pattern of the (0, 4) necklace nanotube is shown in figure 8. The height of the ‘pearls’ is  $p = 0.65$  nm; this periodic repetition gives rise to horizontal layer lines in reciprocal space, with repeat distance  $2\pi/p$ . The first two lines on both sides of the central line of the diffraction pattern have a strong intensity. A similar pattern, with however noticeable intensity differences, is found for the (2,  $-2$ ) nanotube, which has a double-screw structure. In projection in a plane containing the axis, the (2,  $-2$ ) nanotube resembles a necklace with a similar pseudo-period as for (0, 4). This explains the layer lines in the diffraction pattern shown in figure 8. The largest intensities are located close to lines inclined at  $\sim 40^\circ$  from the horizontal direction, which meet close to the left and right ends of the central line.

STM does not help to resolve the atomic structure of the Haeckelite nanotube. Indeed, computed STM images of the Haeckelite (3, 3) and (0, 4) nanotubes [23] demonstrate that it would be impossible to recognize the atomic structure of a Haeckelite nanotube from its STM topography. The number of pentagons and heptagons is so large in these nanotubes that the electronic densities of states are deeply perturbed. The perturbation is not evenly distributed on the atoms, so the imaged atomic structure is masked by the electronic effects [23]. In another but similar context, calculations of the STM image of zig-zag and armchair nanotube tapers, realized by a series of pentagon–heptagon pairs, show that it is impossible to recognize the atomic structure of the nanotube from the topographic image [42].

## 5. Conclusion

To summarize, Haeckelite nanotubes present a rich variety of shapes, perhaps as rich as the variety of C tubular structures produced by CVD. Haeckelite nanotubes provide us with suitable models for coiled, multiple-screw and necklace-like C nanostructures observed experimentally. Electron diffraction and STM do not allow for a clear and direct identification of the possible Haeckelite structure of a nanotube. Nevertheless, the absence of hexagonal arrangements of spots in diffraction and the absence of resolved honeycomb topography in STM indicate that the nanotube does contain a large proportion of non-hexagonal rings.

## Acknowledgments

This work has been partly funded by the IUAP research project P5/01 on ‘Quantum size effects in nanostructured materials’ of the Belgian Office for Scientific, Technical and Cultural Affairs. This work has also benefited from financial support from the Belgian FNRS and the Hungarian Academy of Sciences. Financial support from EU5 Center of Excellence ICAI-CT-2000-70029 and by Hungarian OTKA Grant T 043685 is acknowledged.

## References

- [1] Terrones H, Terrones M, Hernandez E, Grobert N, Charlier J C and Ajayan P M 2000 *Phys. Rev. Lett.* **84** 1716
- [2] Crespi V H, Benedict L X, Cohen M L and Louie S G 1996 *Phys. Rev. B* **53** R13303
- [3] Terrones M, Hsu W K, Hare J P, Kroto H W, Terrones H and Walton D R M 1996 *Phil. Trans. R. Soc. A* **354** 2025  
Terrones M and Terrones H 1996 *Full. Sci. Technol.* **4** 517
- [4] Kroto H W 1988 *Nature* **331** 328
- [5] Iijima S, Ichihashi T and Ando Y 1992 *Nature* **356** 776
- [6] Krishnan A, Dujardin E, Treacy M M J, Hugdahl J, Lynam S and Ebbesen T W 1997 *Nature* **388** 451
- [7] Iijima S, Yudasaka M, Yamada R, Bandow S, Suenaga K, Kokai F and Takahashi K 1999 *Chem. Phys. Lett.* **309** 165
- [8] Weldon D N, Blau W J and Zandbergen H W 1995 *Chem. Phys. Lett.* **241** 365
- [9] Scuseria G E 1992 *Chem. Phys. Lett.* **195** 534
- [10] Dunlap B I 1992 *Phys. Rev. B* **46** 1933
- [11] Dunlap B I 1994 *Phys. Rev. B* **50** 8134
- [12] Stone A J and Wales D J 1986 *Chem. Phys. Lett.* **128** 501
- [13] Monthieux M 2002 *Carbon* **40** 1809
- [14] Saito R, Dresselhaus G and Dresselhaus M S 1996 *Phys. Rev. B* **53** 2044
- [15] Ouyang M, Huang J L and Lieber C M 2001 *Science* **291** 97
- [16] Kim H, Lee J, Kahng S J, Son Y W, Lee S B, Lee C K, Ihm J and Young K 2003 *Phys. Rev. Lett.* **90** 216107
- [17] Ihara S, Itoh S and Kitakami J I 1993 *Phys. Rev. B* **48** 5643
- [18] Amelinckx S, Zhang X B, Bernaerts D, Zhang X F, Ivanov V and B.Nagy J 1994 *Science* **265** 635
- [19] Zhang M, Nakayama Y and Pan L 2000 *Japan. J. Appl. Phys.* **39** L1242
- [20] Gao R, Wang Z L and Fan S 2000 *J. Phys. Chem. B* **104** 1227
- [21] László I and Rassat A 2001 *Int. J. Quantum Chem.* **84** 136
- [22] Biró L P, Márk G I, Koós A A, B.Nagy J and Lambin Ph 2002 *Phys. Rev. B* **66** 165405
- [23] Lambin Ph, Márk G I and Biró L P 2003 *Phys. Rev. B* **67** 205413
- [24] Ajayan P M, Colliex C, Bernier P and Lambert J M 1993 *Microsc. Microanal. Microstruct.* **4** 501
- [25] Akagi K, Tamura R and Tsukada M 1996 *Phys. Rev. B* **54** 14713

- [26] Lauginie P and Conard J 1997 *J. Phys. Chem. Solids* **58** 1949
- [27] Buongiorno Nardelli M, Yakobson B I and Bernholc J 1998 *Phys. Rev. Lett.* **81** 4656
- [28] Yakobson B I 1998 *Appl. Phys. Lett.* **72** 918
- [29] Tersoff J 1988 *Phys. Rev. Lett.* **61** 2879
- [30] Brenner D W 1990 *Phys. Rev. B* **42** 9458
- [31] Robertson D H, Brenner D W and Mintmire J W 1992 *Phys. Rev. B* **45** 12592
- [32] Biró L P, Márk G I, Horváth Z E, Kertész K, Gyulai J, Gruenberger Th, Fulcheri L, B.Nagy J and Lambin Ph 2003 *Carbon* at press
- [33] László I and Rassat A 2003 *J. Chem. Inf. Comput. Sci.* **43** 519
- [34] Zhang X B, Zhang X F, Bernaerts D, Van Tendeloo G, Amelinckx S, Van Landuyt J, Ivanov V, B.Nagy J, Lambin Ph and Lucas A A 1994 *Europhys. Lett.* **27** 141
- [35] Lambin Ph, Fonseca A, Vigneron J P, B.Nagy J and Lucas A A 1995 *Chem. Phys. Lett.* **245** 85
- [36] Zhang X F and Zhang Z 1995 *Phys. Rev. B* **52** 5313
- [37] Akagi K, Tamura R and Tsukada M 1996 *Phys. Rev. B* **53** 2114
- [38] Su C J, Hwang D W, Lin S H, Jin B Y and Hwang L P 2002 *Phys. Chem. Commun.* **5** 34
- [39] Ding D Y, Wang J N, Cao Z L, Dai J H and Yu F 2003 *Chem. Phys. Lett.* **371** 333
- [40] Blank V D, Gorlova I G, Hutchison J L, Kiselev N A, Ormont A B, Polyakov E V, Sloan J, Zakharov D N and Zybtsev S G 2000 *Carbon* **38** 1217
- [41] Amelinckx S, Lucas A A and Lambin Ph 1999 *Rep. Prog. Phys.* **62** 1471
- [42] Meunier V, Buongiorno Nardelli M, Roland C and Bernholc J 2001 *Phys. Rev. B* **64** 195419